Parameter Estimation of Coupled Polynomial Phase and Sinusoidal FM Signals

Djurovic, I.; Wang, P.; Simeunovic, M.; Orlik, P.V.

Abstract

This paper considers parameter estimation of a new coupled mixture of polynomial phase signal (PPS) and sinusoidal frequency modulated (FM) signal, recently introduced for industrial systems such as linear electromagnatic encoders. Compared with both conventional PPS-only and independent mixture models, the coupled mixture one captures the coupling between the sinusoidal FM frequency and the PPS parameters induced by structural system configurations. In this paper, we are particularly interested in estimating phase parameters of the coupled mixture signal at low signal-to-noise ratios (SNRs). Specifically, we propose a three-stage approach consisting of instantaneous frequency (IF) extraction (e.g., the short-time Fourier transform) and refining steps that reduce the bias introduced by the IF estimation and the mean-squared errors (MSEs) up to the Cramer-Rao bound (CRB). The proposed method is numerically compared with an existing phase-based approach as well as corresponding CRBs in terms of the empirical MSE. The results show that, compared with the phase-based approach, the proposed method can significantly lower the SNR threshold. The convergence of the measured MSEs from the initial stage to the latter refining stages is also numerically evaluated.

Signal Processing

Parameter Estimation of Coupled Polynomial Phase and Sinusoidal FM Signals

Igor Djurović[a,b,*], Pu Wang[c], Marko Simeunović[b,d], Philip V. Orlik[c]

[a]*University of Montenegro, 81000 Podgorica, Montenegro (e-mail: igordj@ac.me)*
[b]*Institute for Cutting Edge Information and Communication Technologies, 81000 Podgorica, Montenegro*
[c]*Mitsubishi Electric Research Laboratories (MERL), Cambridge, MA 02139, USA (e-mail: {pwang, porlik}@merl.com)*
[d]*University of Donja Gorica, 81000 Podgorica, Montenegro (e-mail: marko.simeunovic@udg.edu.me)*

Abstract

This paper considers parameter estimation of a new coupled mixture of polynomial phase signal (PPS) and sinusoidal frequency modulated (FM) signal, recently introduced for industrial systems such as linear electromagnatic encoders. Compared with both conventional PPS-only and independent mixture models, the coupled mixture one captures the coupling between the sinusoidal FM frequency and the PPS parameters induced by structural system configurations. In this paper, we are particularly interested in estimating phase parameters of the coupled mixture signal at low signal-to-noise ratios (SNRs). Specifically, we propose a three-stage approach consisting of instantaneous frequency (IF) extraction (e.g., the short-time Fourier transform) and refining steps that reduce the bias introduced by the IF estimation and the mean-squared errors (MSEs) up to the Cramér-Rao bound (CRB). The proposed method is numerically compared with an existing phase-based approach as well as corresponding CRBs in terms of the empirical MSE. The results show that, compared with the phase-based approach, the proposed method can significantly lower the SNR threshold. The convergence of the measured MSEs from the initial stage to the latter refining stages is also numerically evaluated.

Keywords:

Parameter estimation, polynomial phase signal, frequency modulation, coupled mixture signals, time-frequency analysis.

---

*Corresponding author
Email address:* `igordj@ac.me` (Igor Djurović)

1. Introduction

Parameter estimation of *pure* polynomial phase signals (PPSs) from a finite number of samples is a fundamental problem in many applications, including radar, sonar, communications, acoustics and optics [1–17]. A generalized signal model is an *independent* mixture of PPS and sinusoidal frequency modulated (FM) signal referred to as the hybrid sinusoidal FM-PPS [18–23]. One motivation for studying this kind of signal comes from Doppler radar systems. When a target is moving in a dynamic motion, the resulting signal can be modeled as the pure PPS with parameters associated to the kinematic target parameters. For instance, the initial velocity and acceleration are proportional to the first- and second-order phase parameters, respectively. On the other hand, rotating parts (e.g., rotating blades of a helicopter) and target vibration introduce the sinusoidal FM component [18–20]. With both effects, the matched filter outputs follow the independent mixture signal model.

Motivated by real-world applications, e.g., contactless electromagnetic (EM) encoders, a new *coupled* mixture model of the PPS and sinusoidal FM signal is proposed in [24]. Specifically, the coupling is introduced to express the sinusoidal FM frequency as a function of the PPS parameters. The Cramér-Rao bounds (CRB) for parameter estimation has been established in the same paper. Compared with the independent mixture model, the coupled one can lead to lower bounds for estimating the motion-related PPS parameters as the coupled sinusoidal FM frequency provides additional inference for the PPS parameters. As a first attempt, [25] proposed an instantaneous phase-based method using a phase unwrapping technique followed by a nonlinear coupled least square method, referred to as the PULS. It was shown that the PULS method is unbiased and its estimation performance can approach to the CRB at relatively high signal-to-noise ratio (SNR). However, the PULS method exhibits a high SNR threshold[1] especially for a small number of samples.

In this paper, a parameter estimation method is proposed for the coupled mixture signal at low SNRs. Specifically, we propose a three-stage approach which features an instantaneous frequency (IF) extraction by using the short-time Fourier transform (STFT) and refining stages to reduce the estimation bias introduced

---

[1]The SNR threshold is defined as an SNR value below which the mean-squared error (MSE) of the parameter estimate rapidly deviates from the CRB.

by the initial step and to further push the MSEs towards the CRBs. Moreover, the proposed method is extended to the coupled mixture signal with aliasing spectrum. Further, it is numerically compared with the PULS method via extensive Monte-Carlo simulations. We also show the convergence of the MSEs towards corresponding CRBs when the proposed method moves from the initial stage to the latter refining stages.

The remainder of this paper is organized as follows. Section 2 reviews a specific application which motivates the study of the coupled mixture model, defines the mathematical model, and formulates the problem of interest. Section 3 briefly overviews existing parameter estimation methods and established CRBs. The proposed estimator is introduced in details in Section 4. Numerical examples and performance comparisons are provided in Section 5, followed by a summary in Section 6.

2. A Coupled Mixture Signal Model

This section reviews a specific application that motivates the study of the coupled mixture model and compares it with two existing PPS models.

2.1. Linear EM Encoders

Accurate speed sensing is highly desired in contactless encoder systems used for motion/position monitoring. Among others, optical, electric, magnetic and EM encoders are commonly used in applications such as auto-tuning drives, smart conveyors, and kit motors [26–30]. Compared with other types of encoders, EM encoders may provide robust sensing capability of position and motion in harsh operating environments, e.g., moisture, heat, vibration and smoke.

Referring to Fig. 1 of [24], the EM encoder normally consists of a stationary scale and a moving readhead, or vice versa. The source transceivers are mounted on the moving readhead with a distance of r to the scale platform. Uniformly spaced reflectors, e.g., rectangular bars, are installed on the scale platform to constitute a spatial period with an inter-reflector spacing of h. The position encoding is achieved by observing the same reflected EM signals at two spatial positions which are separated with a distance of h. Finer position encoding is enabled by detecting the phase changes of two spatial positions (with a distance change less

3

than h) with respect to a full radian period of 2π (corresponding to a distance change of h). Generally, the baseband signals reflected from the spatially periodic linear scale can be written as

$$x(d) = Ae^{j2\pi\left[\frac{d}{h} + \sum\limits_{m=1}^{M} b_m \sin\left(\frac{2\pi md}{h} + \phi_m\right) + \psi_0\right]}, \tag{1}$$

where A is the unknown amplitude, d is the axial position index of the moving readhead, $b_m > 0$ and ϕ_m are the modulation index and, respectively, the initial phase of the m-th sinusoidal FM component, M is the number of sinusoidal FM components in the phase, and ψ_0 is the initial phase. The first phase term is due to the phase change proportional to the inter-reflector spacing of h. Meanwhile, the second term is, induced by the spatially periodic reflectors, the motion-related sinusoidal FM component. From (1), we have $x(d) = x(d + lh)$, where l is an integer. That is the moving readhead *sees* exactly the same reflected waveforms at two axial positions which are at a distance of h apart from each other.

With a sampling interval of ΔT and assuming that the readhead moves at an initial velocity of v_0 and an acceleration of a, we can transform the position index to the discrete-time index via $d = v_0 t + at^2/2|_{t=n\Delta T} = v_0 n\Delta T + a(n\Delta T)^2/2, n = n_0, \cdots, n_0 + N - 1$ with n_0 and N denoting the initial sampling index and the number of total samples, respectively. As a result, the discrete-time reflected signal for the constantly accelerating readhead is given as

$$x(n) = Ae^{j2\pi\left[\frac{v_0 n\Delta T + a(n\Delta T)^2/2}{h} + \psi_0\right]}$$
$$\times e^{j\sum\limits_{m=1}^{M} 2\pi\left[b_m \sin\left(2\pi m \frac{v_0 n\Delta T + a(n\Delta T)^2/2}{h} + \phi_m\right)\right]}. \tag{2}$$

Note that the sinusoidal FM frequency is now a function of the motion-related phase parameter (e.g., v_0 and a) of the moving readhead.

2.2. The Coupled Mixture of PPS and Sinusoidal FM Signal

For more dynamic motions of the readhead, higher-order phase terms may appear in the reflected signal. For instance, if the acceleration is time-varying, a third-order phase term (on t^3) may be required to model the reflected signal, i.e., $d = v_0 t + at^2/2 + gt^3/6$ where g denotes the acceleration rate. To generalize the

model, a *coupled* mixture of the PPS and sinusoidal FM signal is defined as:

$$x(n) = Ae^{j2\pi \left[\sum_{p=0}^{P} \frac{a_p n^p}{p!} + \sum_{m=1}^{M} b_m \sin(2\pi m f_0(n;\mathbf{a})n + \phi_m) \right]}, \tag{3}$$

where the fundamental sinusoidal FM frequency f_0 is now coupled with the PPS phase parameters $\mathbf{a} \triangleq [a_1, \cdots, a_P]^T$, except the initial phase term a_0. Depending on applications, the coupling function $f_0(n;\mathbf{a})$ can be either nonlinear or linear with respect to $\{a_p\}_{p=1}^{P}$. In the case of linear encoders, we have $f_0(n;\mathbf{a}) = c_0 \sum_{p=1}^{P} a_p n^{p-1}/p!$ with c_0 denoting a *known* scaling factor.

To see how the above example of linear EM encoders fits into the coupled mixture of (3), we can establish the following variable changes between (2) and (3)

$$b_m = b_m, \quad a_0 = \psi_0, \quad a_1 = \frac{v_0 \Delta T}{h}, \quad a_2 = \frac{a(\Delta T)^2}{h}, \tag{4}$$

$$f_0(n;\mathbf{a}) = \frac{v_0 \Delta T}{h} + \frac{a(\Delta T)^2}{h} n/2 = c_0(a_1 + a_2 n/2),$$

with $c_0 = 1$, $\mathbf{a} = [a_1, a_2]^T$, and the PPS order of $P = 2$.

2.3. Comparison of Signal Models

The coupled mixture model given by (3) is distinct from the independent mixture model [18–22]

$$x(n) = Ae^{j2\pi \left[\sum_{p=0}^{P} \frac{a_p n^p}{p!} + \sum_{m=1}^{M} b_m \sin(2\pi m f_0 n + \phi_m) \right]},$$

where the FM frequency f_0 is *independent* of the PPS parameters $\mathbf{a} = [a_1, a_2, \cdots, a_P]^T$. It also generalizes the PPS-only model [1, 3–7, 9, 11–13, 15–17, 31–33]

$$x(n) = Ae^{j2\pi \sum_{p=0}^{P} \frac{a_p}{p!} n^p}$$

as a special case when $b_m = 0$, and $m = 1, \ldots, M$.

2.4. Problem Formulation

The problem of interest here is to estimate the motion-related parameters $\mathbf{a} = [a_1, a_2, \cdots, a_P]^T$ from a finite number of noisy samples of coupled mixture model (3)

$$y(n) = x(n) + \nu(n), n = n_0, n_0 + 1, \cdots, n_0 + N - 1, \tag{5}$$

5

where $x(n)$ is given by (3) and $\nu(n)$ is assumed to be Gaussian noise with zero mean and variance σ^2. With the estimated phase parameters $\{a_p\}_{p=1}^{P}$, one can recover the motion-related parameters, e.g., v_0 and a, via (4). In certain applications, other parameters, e.g., A, $\{b_m\}_{m=1}^{M}$ and ϕ_m, may be of interest as well.

3. Prior Arts

We first review two existing methods for the problem of interest here: 1) the maximum likelihood (ML) estimation and 2) the phase-based PULS estimation [25], and then the established performance bound in terms of the CRB [24].

3.1. MLE: Maximum Likelihood Estimation

The MLE minimizes the following negative log-likelihood function

$$\Lambda = \frac{\sum_n \left| y(n) - A e^{j2\pi \left[\sum_{p=0}^{P} \frac{a_p n^p}{p!} + \sum_m b_m \sin(2\pi m f_0(n;\mathbf{a})n + \phi_m) \right]} \right|^2}{\sigma^2}$$

which gives rise to the ML estimates of the unknown parameters as

$$[\hat{\mathbf{a}}, \hat{\mathbf{b}}, \hat{\boldsymbol{\phi}}] = \arg \max_{[\boldsymbol{\alpha}, \boldsymbol{\beta}, \boldsymbol{\xi}]} J(\boldsymbol{\alpha}; \boldsymbol{\beta}; \boldsymbol{\xi}) \tag{6}$$

where $\mathbf{a} = [a_1, \cdots, a_P]^T$, $\mathbf{b} = [b_1, \cdots, b_M]^T$, $\boldsymbol{\phi} = [\phi_1, \cdots, \phi_M]^T$ and the cost function $J(\boldsymbol{\alpha}; \boldsymbol{\beta}; \boldsymbol{\xi})$ is defined as:

$$J(\boldsymbol{\alpha}; \boldsymbol{\beta}; \boldsymbol{\xi}) = \left| \sum_n y(n) \exp \left(-j2\pi \sum_{p=1}^{P} \frac{\alpha_p n^p}{p!} \right. \right. \tag{7}$$
$$\left. \left. -j2\pi \sum_{m=1}^{M} \beta_m \sin(2\pi m f_0(n; \boldsymbol{\alpha})n + \xi_m) \right) \right|^2.$$

It is seen that the MLE of (7) is a generalization of the FFT-based spectrum estimation. Specifically, when $\beta_m = 0$ and $P = 1$, the MLE reduces to the squared magnitude of the FFT of the measured signal. However, to find all these parameters, the MLE is a function of $(2M+P)$ parameters and, hence, a $(2M+P)$-dimensional search over the parameter space is required and, hence, it is computationally prohibited from practical applications. Hence, optimization is usually done using some iterative approaches. Due to the

6

high-order non-linearity of (7), the optimization procedure may converge to a local minimum if initial guess is far away from the global minimum. It has been shown in [32] that even meta-heuristic techniques such are genetic algorithms are unable to converge for more than 5-dimensional search space.

3.2. PULS: Phase Unwrapping and Nonlinear Least Square

Introduced in [25] for the linear encoder application, the PULS method is a computationally lighter approach than the MLE method. As summarized in Fig. 1, it first extracts the instantaneous phase from $y(n)$ by the phase unwrapping technique, and then estimates the motion-related phase parameters from the extracted phase by a coupled least square fitting.

3.2.1. Phase Unwrapping

The first step is to extract the phase of the sampled signal and unwrap it using the phase unwrapping technique

$$
\begin{aligned}
\hat{\phi}(n) &= \frac{\text{unwrap}(\text{phase}(y(n)))}{2\pi} \\
&= \sum_{p=0}^{P} \frac{\alpha_p n^p}{p!} + \sum_{m=1}^{M} b_m \sin(2\pi m f_0(n; \mathbf{a})n + \phi_m) + w(n),
\end{aligned}
\tag{8}
$$

where $n = n_0, \cdots, n_0 + N - 1$ and $w(n)$ is the noise contribution to the unwrapped phase.

3.2.2. Nonlinear Least Square

From (8), it is seen that the motion-related parameters, i.e., $\mathbf{a} = [a_1, a_2, \cdots, a_P]^T$, are present in the unwrapped phase. More precisely, they appear in both the first term as *linear* variables and the second term as *nonlinear* variables via the sinusoidal frequency $f_0(n; \mathbf{a})$. Then, the unknown parameters in (8) can be subsequently estimated from the nonlinear least square method; see Section III.B of [25] for the details.

The PULS estimator was shown to work well at high SNRs with the MSE approaching to the corresponding CRB. However, its performance is quickly degraded at low SNRs (see numerical examples in Section 5). Moreover, due to the coupling effect, the phase variation becomes more rapid which may cause additional errors from the phase unwrapping step. Besides, the aliasing effect, overwhelming with respect to the PPS-only and independent mixture models, has not been addressed in [25].
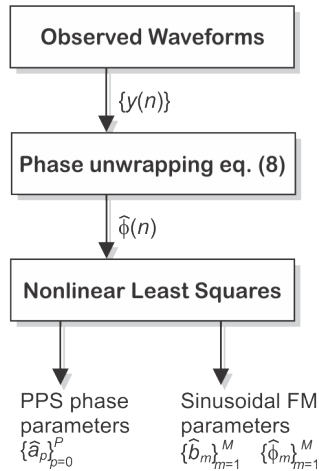
```
┌─────────────────────────┐
│   Observed Waveforms    │
└─────────────────────────┘
            │ {y(n)}
            ▼
┌─────────────────────────┐
│ Phase unwrapping eq. (8)│
└─────────────────────────┘
            │ φ̂(n)
            ▼
┌─────────────────────────┐
│ Nonlinear Least Squares │
└─────────────────────────┘
        │           │
        ▼           ▼
  PPS phase     Sinusoidal FM
  parameters    parameters
  {âₚ}ᴾₚ₌₀      {b̂ₘ}ᴹₘ₌₁  {φ̂ₘ}ᴹₘ₌₁
```

Figure 1: The flowchart of the phase-based PULS method in [25].

3.3. Performance Bound: Cramér-Rao Bound

The CRBs for the parameter estimates of the coupled mixture model have been derived in [24]. It reveals that, on one hand, the CRB is dependent on both PPS- and sinusoidal FM-related phase parameters, an observation that is different from the case of the PPS-only model. On the other hand, the derived CRBs for the PPS-related parameters are lower than their counterparts of the independent mixture model, as the sinusoidal FM frequency provides additional inference on the PPS-related parameters.

4. Proposed Estimator

4.1. Description and Motivation

The phase unwrapping techniques are known to be accurate when phase of narrowband signals at high SNRs are reconstructed. However, their performance deteriorates in the cases of fast phase variations and wideband signals or when the noise is strong. Our purpose here is to address these remaining issues of the phase-based PULS method and enhance its performance in these unfavored conditions.

For the PPS-only model, there are latest efforts to combine computationally efficient but biased estimators at earlier stages for initial estimates located close enough to the global minimal of the MLE, and then refine the biased estimates towards the CRB at latter stages [34]. One of such efforts for the PPS-only model is the quasi maximum likelihood (QML) method [35–38]. It first obtains initial estimates of the PPS phase

8

parameters by using a polynomial regression on the biased IF estimates from the spectrogram (squared magnitude of the STFT). The polynomial regression is fast with a closed-form solution as the IF is linear with respect to the PPS phase parameters. Then the original sampled signal is dechirped (demodulated) with these initial parameter estimates and low-pass filtered to reduce the out-of-band noise. It was shown that, with the dechirping and low-pass filtering operations, the resulting signal is narrowband around the DC frequency, allowing for a more stable and accurate phase unwrapping, compared with the case of phase unwrapping directly on the original wideband signal. More importantly, the dechirped and filtered signal can still be approximated by a PPS-only model but with an offset parameter introduced to each of the original PPS phase parameters. These offset parameters can be estimated by, again, the fast polynomial regression on the unwrapped phase of the resulting narrowband signal. Finally, the offset estimates are used to compensate the initial parameter estimates to reduce the estimation bias and converge the estimation performance towards the CRB.

For the coupled mixture signal considered here, on one hand, a direct application of the QML method may fail since the phase parameters are not only embed *linearly* in the PPS-related IF (similar to the PPS-only case), but also *non-linearly* in the sinusoidal FM-related IF due to the coupling. On the other hand, if one fully takes into account the presence of the nonlinear sinusoidal FM component for the initial estimates as well as for the refined estimates, a multi-dimensional nonlinear search is required and the resulting computational complexity is still too high. As a result, we propose a three-stage parameter estimation method by adopting the principle of the QML in the context of the coupled mixture signal with a computationally much more efficient way.

4.2. Initial Phase Parameter Estimates

The initial stage is to obtain reliable phase parameter estimates which are likely biased but not far away from the global minimal. These initial estimates can be further improved and refined by the latter stages. It is known that the time-frequency representations are robust to the noise influence with many well developed techniques for the IF estimation [39–43]. Compared with bilinear transforms, linear transforms are more robust to the noise by paying the price of estimation bias [39]. Particularly, the STFT-based IF estimator is

highly influenced by the window size. The bias is larger when the window size increases, while the variance decreases due to the larger number of samples.

Particularly, the initial parameter estimates can be obtained in the following steps:

Step 1. *Estimation of the IF $\omega(n)$* by maximizing the the magnitude of the STFT:

$$\hat{\omega}(n) = \arg \max_{\omega} |\text{STFT}(n, \omega)|, \tag{9}$$

$$\text{STFT}(n, \omega) = \sum_k w_g(k) y(n+k) e^{-j\omega k}, \tag{10}$$

where $w_g(k)$ is a (rectangular) window function with $w_g(k) = 1$ for $k \in [-g/2, g/2]$ and $w_g(k) = 0$, elsewhere, and g is the chosen window size. It is possible to compute the STFT with different window sizes [35] to reduce the estimation bias in the IF estimates. For the sake of computational complexity, only one window size is used here.

Step 2. *Polynomial interpolation of the estimated IF* resulting in initial PPS parameter estimates $\{\hat{a}'_p | p \in [1, P]\}$:

$$\hat{\mathbf{a}} = (\mathbf{\Gamma}^T \mathbf{\Gamma})^{-1} \mathbf{\Gamma}^T \mathbf{\Omega}, \tag{11}$$

where the elements of $\mathbf{\Omega}$ are samples of IF estimates $\hat{\omega}(n)$, and the elements of the $N \times P$ matrix $\mathbf{\Gamma}$ are given as $\mathbf{\Gamma}_{i,p} = 2\pi \frac{i^{p-1}}{(p-1)!}$, $i \in [n_0, n_0 + N - 1]$ and $p \in [1, P]$.

Step 3. *Estimation of the sinusoidal FM parameters* based on the above estimated IF and PPS parameters. Note that, in Step 2, we still use a simple polynomial regression for the initial estimates of $\{a_p\}_{p=1}^P$ by ignoring the sinusoidal FM component. The parameters associated with the sinusoidal FM component are then estimated by reconstructing the PPS-related IF using the initial estimates of $\{a_p\}_{p=1}^P$ in (11) and subtracting it from the estimated IF in (9). More precisely, we define the following variable

$$\gamma(n) = \frac{\hat{\omega}(n) - 2\pi \sum_{p=1}^P \frac{\hat{a}'_p n^{p-1}}{(p-1)!}}{4\pi^2 [f_0(n; \hat{\mathbf{a}}) + \frac{\partial f_0(n; \hat{\mathbf{a}})}{\partial n}]}, \tag{12}$$

where the numerator is an IF estimate for the sinusoidal FM component by subtracting the reconstructed PPS-related IF from the overall estimated IF, and the denominator includes the sinusoidal

FM-related IF terms only associated to $\{a_p\}_{p=1}^P$ which are replaced by the initial estimates $\{\hat{a}_p'\}_{p=1}^P$ in (11). As a result, $\gamma(n)$ can be approximated as

$$
\begin{aligned}
\gamma(n) &\approx \sum_{m=1}^M m b_m \cos(2\pi m f_0(n; \widehat{\mathbf{a}})n + \phi_m) \\
&= \sum_{m=1}^M m b_m \cos(2\pi m f_0(n; \widehat{\mathbf{a}})n) \cos \phi_m \\
&\quad - \sum_{m=1}^M m b_m \sin(2\pi m f_0(n; \widehat{\mathbf{a}})n) \sin \phi_m \\
&\triangleq \sum_{m=1}^M m b_m^c c(n; m) - \sum_{m=1}^M m b_m^s s(n; m),
\end{aligned}
\tag{13}
$$

where $b_m^c = b_m \cos \phi_m$, $b_m^s = b_m \sin \phi_m$, $c(n; m) = \cos(2\pi m f_0(n; \widehat{\mathbf{a}})n)$, and $s(n; m) = \sin(2\pi m f_0(n; \widehat{\mathbf{a}})n)$. Subsequently, we can rewrite (13) in a vector-matrix form as

$$
\begin{aligned}
\boldsymbol{\gamma} &= [\gamma(n_0), \cdots, \gamma(n_0 + N - 1)]^T \\
&= \mathbf{C}\mathbf{b}_c + \mathbf{S}\mathbf{b}_s
\end{aligned}
\tag{14}
$$

where $\mathbf{b}_c = [b_1^c, \cdots, b_M^c]^T$, $\mathbf{b}_s = [b_1^s, \cdots, b_M^s]^T$ and

$$
[\mathbf{C}]_{\ell,m} = m \cdot c(n_0 + \ell - 1, m), m = 1, \cdots, M,
$$

$$
[\mathbf{S}]_{\ell,m} = m \cdot s(n_0 + \ell - 1, m), \ell = 1, \cdots, N.
$$

Then, the $2M$ parameters $\mathbf{b}_c = \{b_m^c\}$ and $\mathbf{b}_s = \{b_m^s\}$ can be estimated as a linear least square solution

$$
\begin{bmatrix} \hat{\mathbf{b}}_c \\ \hat{\mathbf{b}}_s \end{bmatrix} = \left([\mathbf{C}, \mathbf{S}]^T [\mathbf{C}, \mathbf{S}]\right)^{-1} [\mathbf{C}, \mathbf{S}]^T \boldsymbol{\gamma}.
\tag{15}
$$

Note that, since $N \gg M$, the above linear least square solution is well poised. Finally, the $2M$ phase parameters b_m and ϕ_m associated with the sinusoidal FM component can be estimated from $\hat{b}_m^c$ and $\hat{b}_m^s$,

$$
\hat{b}_m' = \sqrt{(\hat{b}_m^c)^2 + (\hat{b}_m^s)^2},
\tag{16}
$$

$$
\hat{\phi}_m' = \arctan \frac{\hat{b}_m^s}{\hat{b}_m^c}.
\tag{17}
$$

When $\phi_1 = \phi_2 = \cdots = \phi_M = \phi$, $\hat{\phi}'$ can be averaged out over the M estimates of $\hat{\phi}'_m$,

$$\hat{\phi}' = \frac{1}{M} \sum_{m=1}^{M} \arctan \frac{\hat{b}^s_m}{\hat{b}^c_m}.$$

In a short summary, we have obtained the initial estimates of all phase parameters from (11), (16), and (17) all in closed-form solutions.

4.3. Dechirping and Low-Pass Filtering

The initial phase parameter estimates suffer from the estimation bias due to the STFT. In this stage, we employ the dechirping operation to compress the original sampled signal into a narrowband signal around the DC frequency, and the low-pass filtering to suppress the out-of-band noise. Since the resulting signal is narrowband, we apply the phase unwrapping technique to extract its phase and compensate it back to the reconstructed phase with these initial phase parameter estimates.

First, we reconstruct the signal with the above initial estimates

$$\hat{x}(n) = e^{j2\pi \left(\sum_{p=1}^{P} \frac{\hat{a}'_p n^p}{p!} + \sum_{m=1}^{M} \hat{b}'_m \sin(2\pi m f_0(n;\hat{\mathbf{a}})n + \hat{\phi}'_m) \right)}, \tag{18}$$

and dechirp the original sampled signal with the reconstructed signal as

$$\tilde{y}(n) = y(n)\hat{x}^*(n). \tag{19}$$

It is expected that, given relatively accurate initial estimates, the resulting dechirped signal is narrowband and its spectrum is around the DC frequency. Fig. 2 shows spectra of the original sampled signals $y(n)$ and the dechirped signal $\tilde{y}(n)$ in (19) with initial estimates from the STFT-based spectrogram calculated using window size of 24 samples. The sampled signal is the same as the one used in Section 5.4. One can notice the wideband nature of the considered coupled mixture signal and the narrowband of the dechirped signal.

To reduce the out-of-band noise, the dechirped signal $\tilde{y}(n)$ is further filtered by a low-pass moving average (MA) filter

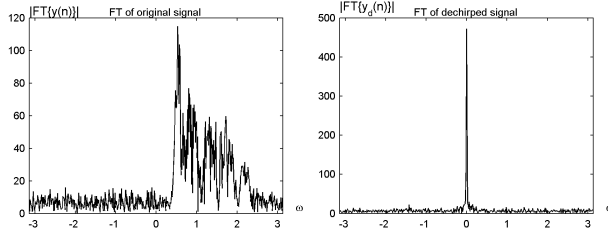$$\hat{y}(n) = \frac{1}{2L+1} \sum_{l=-L}^{L} \tilde{y}(n+l), \tag{20}$$

12

Figure 2: Spectra of a noisy coupled mixture signal $y(n)$, the same one used in Section 5.4, and the dechirped signal $\tilde{y}(n)$ of (19) using initial estimates from the STFT-based spectrogram with a window size of 24 samples.

where $2L+1$ is the filter length. As a result, $\hat{y}(n)$ is narrowband with an enhanced SNR. Consequently, the phase unwrapping technique is now reliable to extract the phase of the resulting signal which contains the phase offset between the true and reconstructed phase from the initial estimates,

$$v(n) = \text{unwrap}(\text{phase}(\hat{y}(n))). \tag{21}$$

With $v(n)$, the refined estimate $\hat{\phi}(n)$ of the original phase can be obtained from two parts: 1) the reconstructed phase from the initial estimates obtained at the initial stage; and 2) the unwrapped phase $v(n)$ of the dechirped and low-pass filtered signal $\hat{y}(n)$. Specifically, the refined phase estimate $\hat{\phi}(n)$ is given as

$$\begin{aligned}\hat{\phi}(n) =& 2\pi \sum_{p=1}^{P} \frac{\hat{a}'_p n^p}{p!} \\ & + 2\pi \sum_{m=1}^{M} \hat{b}'_m \sin(2\pi m f_0(n; \hat{\mathbf{a}})n + \hat{\phi}'_m) + v(n).\end{aligned} \tag{22}$$

4.4. Refining Phase Parameter estimation

Now we need to refine the PPS-related and sinusoidal FM-related parameter estimates from the above refined phase estimate $\hat{\phi}(n)$ of (22). For the sake of computational complexity, the parameter refining stage takes a two-step closed-form solution. First, we refine the estimates of the parameters $\{\hat{a}''_p | p \in [0, P]\}$ by using the polynomial regression on $\hat{\phi}(n)$:

$$\widehat{\hat{\mathbf{a}}} = (\mathbf{\Xi}^T \mathbf{\Xi})^{-1} \mathbf{\Xi}^T \boldsymbol{\phi} \tag{23}$$

where the n-th element of $\boldsymbol{\phi}$ is the phase estimate $\hat{\phi}(n)$, the elements of $N \times (P+1)$ matrix $\mathbf{\Xi}$ are $\xi_{i,p} = \frac{2\pi i^p}{p!}$, $i \in [n_0, n_0 + N - 1]$ and $p \in [0, P]$, and the vector $\widehat{\hat{\mathbf{a}}}$ groups the refined estimates of the parameters $\hat{a}''_p$,

13

$p \in [0, P]$.

To refine the remaining sinusoidal FM-related parameters, we remove the contribution of the reconstructed PPS-related phase using the refined estimates $\hat{a}_p''$

$$\Delta\phi(n) = \hat{\phi}(n) - 2\pi \sum_{p=0}^{P} \frac{\hat{a}_p'' n^p}{p!}. \tag{24}$$

Similar to (13), $\Delta\phi(n)$ may be expressed as

$$\begin{aligned}
\Delta\phi(n) =& 2\pi \sum_{m=1}^{M} b_m \sin(2\pi m f_0(n; \widehat{\hat{\mathbf{a}}})n + \phi_m'') + v(n) \\
=& 2\pi \sum_{m=1}^{M} [b_m \sin(2\pi m f_0(n; \widehat{\hat{\mathbf{a}}})n) \cos\phi_m'' \\
& + b_m \cos(2\pi m f_0(n; \widehat{\hat{\mathbf{a}}})n) \sin\phi_m''] \\
=& 2\pi \sum_{m=1}^{M} [b_m^c s(n; m) + b_m^s c(n, m)], \tag{25}
\end{aligned}$$

where the refined estimates $\hat{b}_m''$ and $\hat{\phi}_m''$ can be obtained with a similar linear least square solution given by (16) and (17) of Section 4.2.

Finally, these phase parameter estimates can be further improved by minimizing the cost function of (7) with these refined parameters $\boldsymbol{\alpha} = \widehat{\hat{\mathbf{a}}}$, $\boldsymbol{\beta} = \{\hat{b}_m''\}_{m=1}^{M}$, and $\boldsymbol{\xi} = \{\hat{\phi}_m''\}_{m=1}^{M}$.

4.5. Algorithm Implementation

As shown in Fig. 3, the step-by-step implementation for the proposed method is summarized below:

Stage 1. *Preparatory Stage*

1.a) Compute the STFT using (10) with a chosen window size;

1.b) Estimate the IF, $\hat{\omega}(n)$, by (9).

Stage 2. *Initial Phase Parameter Estimates*

2.a) Perform the polynomial regression on $\hat{\omega}(n)$ to obtain $\{\hat{a}_p' | p \in [1, P]\}$ from (11);

2.b) Estimate $\hat{b}_m'$ and $\hat{\phi}_m'$ using (16) and (17).

Stage 3. *Refined Phase Parameter Estimates*

3.a) Reconstruct the signal with the above initial phase parameter estimates according to (18);

14
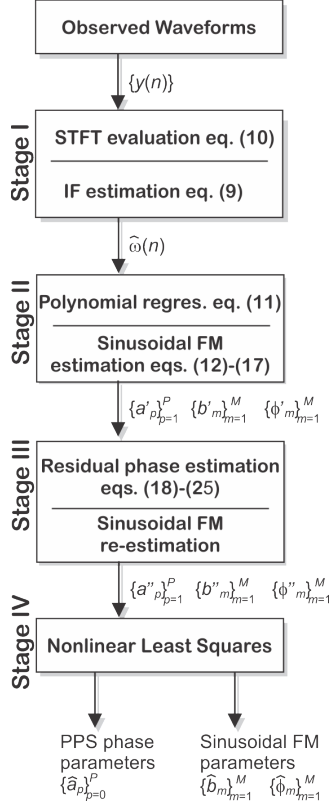
Figure 3: The flowchart of the proposed estimator.

3.b) Dechirp (demodulate) the original sample signal according to (19);

3.c) Perform the low-pass (moving average) filtering according to (20);

3.d) Extract the phase of the resulting narrowband filtered signal in (21);

3.e) Reconstruct the refined phase according to (22);

3.f) Refine the estimates of the phase parameters $\{\hat{a}_p''|p \in [0,P]\}$ according to (23).

3.g) Calculate the residual phase function $\Delta\phi(n)$ in (24).

3.h) Refine the estimate of the phase parameters $\{\hat{b}_m'', \hat{\phi}_m''|m \in [1,M]\}$ as in Stage 2.

Stage 4. *Nonlinear optimization.* The final parameter estimates are obtained by minimizing the cost function of (7) by using the refined phase parameters in Stage 3 as the starting point.

As we pointed out before, the computationally most demanding step is to compute the STFT in the preparatory stage which requires $O(N^2 \log N)$ operations, while other steps of the proposed method can be

implemented with less computational complexity than that of the STFT.

4.6. Effect of Aliasing

The coupled mixture signal can be characterized by the aliasing effect, i.e., signal is sampled below the Nyquist frequency [44]. It is well known that the PPSs are uniquely characterized well below the Nyquist criterion sampling [45, 46]. Such theoretical analysis is not available for the coupled mixture signal but it can be assumed that similar situation holds as for the PPS. The modification of the proposed algorithm for the aliased signals is surprisingly simple with single change in Stage 1.b). For the sampling interval ΔT the frequency domain of the STFT is $\omega \in [-\pi/\Delta T, \pi/\Delta T)$. Then, the IF estimate can be unwrapped as

$$\hat{\omega}_u(n) = \frac{1}{\Delta T} \text{unwrap}(\hat{\omega}(n)\Delta T), \tag{26}$$

using the same unwrap (for example MATLAB) function as used in Stage 3.d. In this way the IF is unwrapped along accurate signal parameters estimation. The other algorithm steps are the same as in the original algorithm. More details on the unwrapping of the IF estimate and application to FM signal parameters estimation can be found in [44].

5. Numerical Results

In this section, we numerically evaluate the empirical MSE of the proposed estimator by Monte-Carlo simulations and compare it with the PULS method of [25] as well as corresponding CRB [24].

5.1. Coupled Mixture of A Chirp Signal ($P = 2$) and A Weak Sinusoidal FM Signal ($M = 1$ and $b = 0.05$)

We first consider a coupled mixture signal of a second-order PPS component ($P = 2$, also referred to as chirp signals) and a weak mono-component sinusoidal FM component ($M = 1$ and small b). Specifically, the coupled mixture signal model of (3) reduces to

$$x(n) = Ae^{j2\pi\left[a_0 + a_1n + a_2n^2/2 + b\sin(2\pi c_0(a_1n + a_2n^2/2) + \phi)\right]}, \tag{27}$$

with parameters given as $A = 1$, $a_0 = 0$, $a_1 = 0.15$, $a_2 = 1.3889 \cdot 10^{-4}$, $b = 0.05$, $c_0 = 0.1$, $\phi = 0$, $N = 512$, $n_0 = -N/2$, and $f_0(n; \mathbf{a}) = c_0(a_1 + a_2n/2)$. For the proposed estimator, we used a single STFT with a

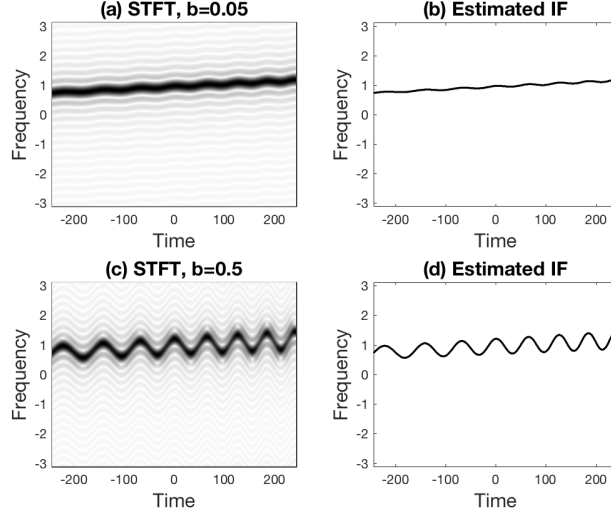Figure 4: STFT spectra and extracted IF for the noiseless coupled mixture of a chirp signal (a-b) and a weak sinusodial FM component ($b = 0.05$) and (c-d) a strong sinusoidal FM component ($b = 0.5$).

window size of 24 samples. The low-pass filtering in the refining stages is performed with a moving average filter with 5 samples ($L = 2$). Complexity of the proposed technique is reasonable. Single trial of the proposed estimator at laptop computer with processor Intel i7-5500U CPU 2.40GHz, with 8GB RAM and MATLAB R2015a takes an average less than 0.14sec for this signal.

Fig. 4 (a) shows the initial STFT spectra with a window size of 24 samples, while Fig. 4 (b) shows the estimated IF from the peak locations. It is seen that the STFT spectra is dominated by the straight line IF of the chirp component with small oscillations introduced by the weak sinusoidal FM component. Fig. 5 shows the evaluated MSEs of the proposed estimator as a function of SNR for the motion-related parameters, i.e., a_2 and a_1, and the sinusoidal FM phase parameters, i.e., b and ϕ. In each plot, we show the convergence of the evaluated MSEs from the early stage to the final refining stage. It is clear that, especially for the estimates of a_2, a_1, and b, the estimation bias is dominant at earlier stages (e.g., Stage 2) as the MSEs flatten out, a strong indicator of the bias. The refining stages (e.g., Stage 4) then successfully remove the estimation bias and move the MSE approaching to the corresponding CRB (denoted as red solid lines).

Meanwhile, the MSEs of the proposed estimator are compared with those of the PULS estimator of [25].
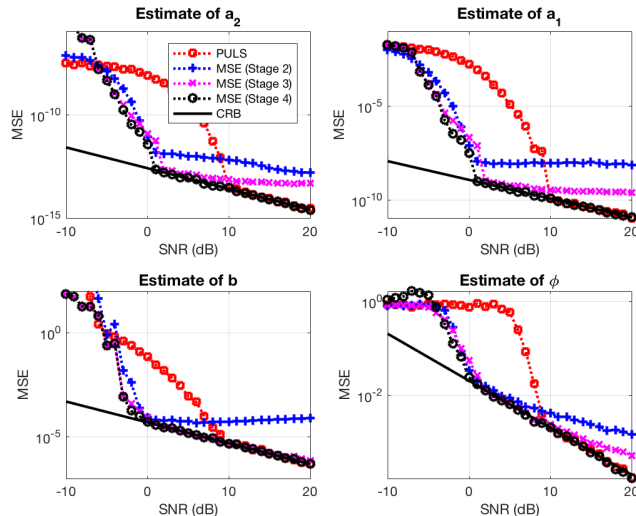
Figure 5: Comparison of measured MSEs for the parameter estimation of the coupled mixture of a chirp signal ($P = 2$) and a weak sinusoidal FM signal ($M = 1$ and $b = 0.05$).

It is seen that the PULS estimator is unbiased at high SNR and its estimation performance approaches to the CRB. However, when the SNR is below its SNR threshold, i.e., 10 dB in this case, the MSEs increase significantly and are several order of magnitude larger than of the proposed estimator, which works well at SNRs as lows as 1 dB.

5.2. Coupled Mixture of A Chirp Signal ($P = 2$) and A Strong Sinusoidal FM Signal ($M = 1$ and $b = 0.5$)

Next, we consider the same mixture signal of (27) except that the sinusoidal FM component is stronger by increasing b to $b = 0.5$. The STFT with the window size of 24 samples and the estimated IF from the initial STFT are given in Fig. 4 (c) and (d), respectively. Compared with the previous case, the oscillation of the IF is more visible.

Similarly, the measured MSEs for the four parameters (a_2, a_2, b and ϕ) are shown and compared with those of the PULS estimator as well as corresponding CRBs in Fig. 6. The observations from Fig. 6 are similar to what we already observed from Fig. 5, except that the MSE for estimating ϕ is smaller. Comparing the proposed estimator with the PULS estimator reveals a 9-dB improvement of the SNR threshold. It is also noted that, with a stronger FM component, the MSEs of the proposed method converges slower to the
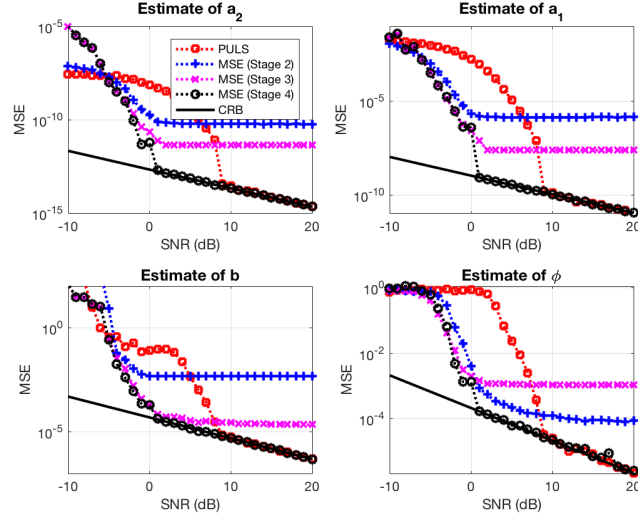
Figure 6: Comparison of measured MSEs for the parameter estimation of the coupled mixture of a chirp signal ($P = 2$) and a strong sinusoidal FM signal ($M = 1$ and $b = 0.5$).

CRB.

5.3. Coupled Mixture of A Third-Order PPS ($P = 3$) and A Weak Sinusoidal FM Signal ($M = 1$ and $b = 0.05$)

We then consider a coupled mixture signal of a third-order PPS ($P = 3$) and a weak mono-component sinusoidal FM ($M = 1$ and small b). In this case, the coupled mixture signal model of (3) reduces to

$$x(n) = A e^{j2\pi[a_0 + a_1 n + a_2 n^2/2 + a_3 n^3/6]}$$

$$\times\, e^{j2\pi b \sin(2\pi c_0(a_1 n + a_2 n^2/2 + a_3 n^3/6) + \phi)}, \tag{28}$$

with parameters given as $A = 1$, $a_0 = 0$, $a_1 = 0.08$, $a_2 = 1.5662 \cdot 10^{-4}$, $a_3 = 0.8022 \cdot 10^{-5}$, $b = 0.05$, $c_0 = 0.1$, $\phi = 0$, $N = 512$, $n_0 = -N/2$, and $f_0(n; \mathbf{a}) = c_0(a_1 + a_2 n/2 + a_3 n^2/6)$.

For this case, Fig. 7 (a) shows the initial STFT spectra with a window size of 24 samples, while Fig. 7 (b) shows the estimated IF from the peak locations. One can observe that the STFT spectra and the extracted IF are shaped mainly by the phase parameters (a_1, a_2 and a_3) of the third-order PPS component with small oscillations added by the sinusoidal FM component.
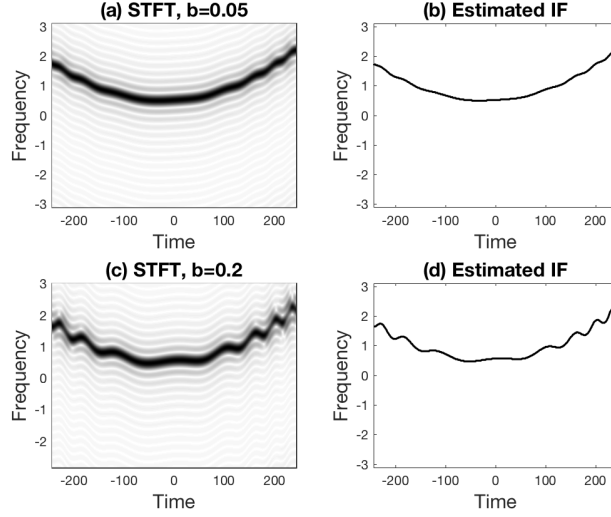
Figure 7: STFT spectra and extracted IF for the noiseless coupled mixture of a third-order PPS (a-b) and a weak sinusoidal FM component ($b = 0.05$) and (c-d) a moderate FM component ($b = 0.2$).
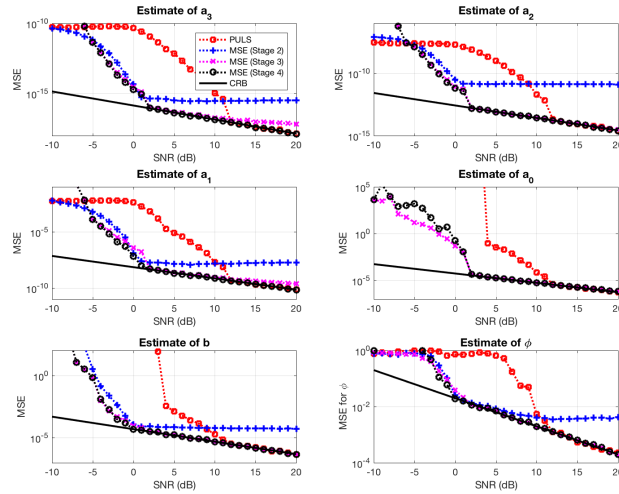

Figure 8: Comparison of measured MSEs for the parameter estimation of the coupled mixture of a third-order PPS ($P = 3$) and a weak sinusoidal FM signal ($M = 1$ and $b = 0.05$).

Fig. 8 presents the measured MSEs from all 6 phase parameters, i.e., $\{a_i\}_{i=0}^3, b$, and ϕ, from the two considered estimators and corresponding CRBs. It is seen that, starting from the third stage (i.e., Stage 3) the proposed estimator is shown to correct the estimation bias at high SNRs from previous stages and give measured MSEs almost approaching to the CRB.

5.4. Coupled Mixture of A Third-Order PPS ($P = 3$) and A Moderate Sinusoidal FM Signal ($M = 1$ and $b = 0.2$)

Next, we increase the sinusoidal FM index to $b = 0.2$ while keeping all other parameters the same. The STFT with the window size of 24 samples and the estimated IF from the initial STFT are given in Fig. 7 (c) and (d), respectively. It is worth noting that, from Fig. 7 (c) and (d), the coupled oscillation pattern at the negative time indices is distinct from that at the positive time indices. In order to demonstrate robustness of the proposed method with respect to the noise we have considered three trials in the parametric estimation of this signal for SNR=20dB, 10dB, and 0dB in Fig. 9. The phase unwrapping of the original signal used for regression in the PULS algorithm is given in Fig. 9(a). It can be seen that there is difference in phase reconstruction for SNR=10dB with respect to SNR=20dB while the phase reconstruction for SNR=0dB is obviously useless in the parameter estimation. Fig. 9(b) depicts the IF estimation for considered three cases using the STFT (10). It can be seen that obtained results are stable even for low SNR. Then dechirping based on the IF estimate (18), (19), together with low-pass filtering (20), create favorable condition for phase unwrapping (21), with reconstructed phase given in Fig. 9(c). The measured MSEs for the two considered methods are shown in Fig. 10 for all the six phase parameters. Comparing Fig. 10 with Fig. 8 shows that the convergence rate of the proposed method is slower with a larger sinusoidal FM index b as the measured MSEs at Stage 3 (denoted as magenta crosses) are still saturated at high SNRs, especially for estimating a_3 and a_1. Again, one can clearly see a 10dB improvement of the SNR threshold.

5.5. The Effect of Initial IF estimate

The robustness of the proposed technique is influenced mainly by the initial algorithm stage with the STFT-based IF estimator. Accuracy of the IF estimator is influenced by the window width used in the
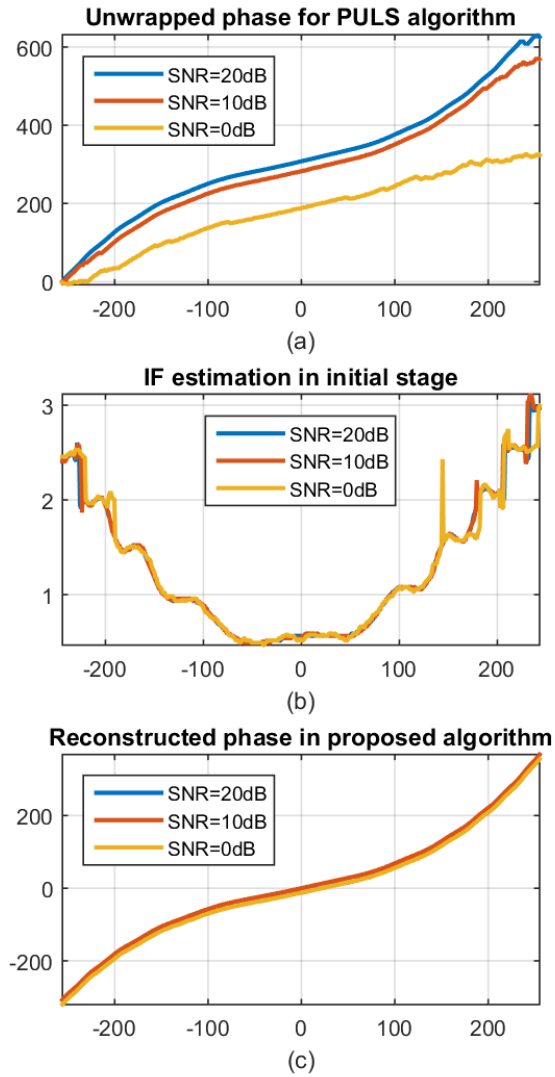
Figure 9: Comparison of the proposed algorithm with the PULS one for three different SNRs: (a) phase unwrapping of noisy signal; (b) IF estimation using STFT; (c) phase reconstruction using proposed algorithm (phase unwrapping of dechirped and filtered signal).
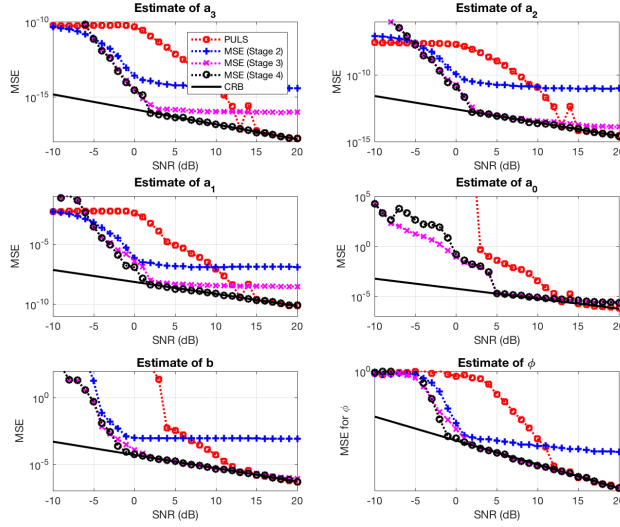
Figure 10: Comparison of measured MSEs for the parameter estimation of the coupled mixture of a third-order PPS ($P = 3$) and a moderate sinusoidal FM signal ($M = 1$ and $b = 0.2$).

STFT. The IF estimate with narrow windows is sensitive to the noise influence while wide windows can cause emphatic bias. For details on the trade-off between bias and variance in the IF estimation refer to [39]. We have used signal from the previous subsection, i.e., third order PPS ($P = 3$) and moderate sinusoidal component $b = 0.2$ and tested accuracy of the proposed technique for windows of the length g between 4 and 48 samples. It can be seen from Fig. 11 (for brevity only MSE in the a_3 estimation is depicted) that for $g \in [24, 48]$ accuracy of the proposed technique is almost the same, achieving the CRB above the SNR threshold of 1dB. Since the IF estimators with narrower windows are prone to the noise influence they exhibit higher SNR thresholds. In addition, the MSE with adaptive selection of window width is given with dashed line. Limited improvement of accuracy is possible in this case so we have used single window length in our simulations in order to reduce calculation complexity.

5.6. The Effect of Aliasing

Finally, we consider the effect of aliasing, i.e., the maximum frequency of the signal is larger than half of the sampling frequency, to the estimation performance of the proposed method. For this purpose, we consider a coupled mixture of (28) with parameters given as $A = 1$, $a_0 = 0$, $a_1 = 0.15$, $a_2 = 1.3889 \cdot 10^{-4}$,
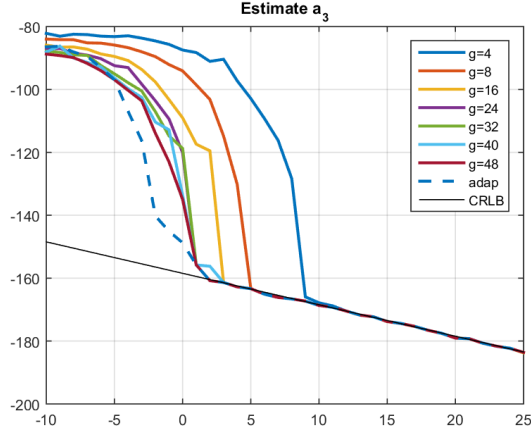
Figure 11: Comparison of measured MSEs for estimation of parameter a of the coupled mixture of a third-order PPS ($P = 3$) and a moderate sinusoidal FM signal ($M = 1$ and $b = 0.2$) for various window lengths in the STFT.
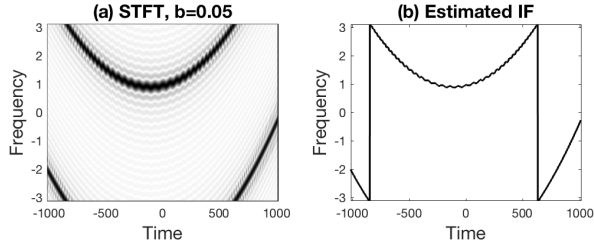

Figure 12: Aliased STFT spectra and extracted IF for a noiseless coupled mixture signal.

$a_3 = 1.3022 \cdot 10^{-6}$, $b = 0.05$, $c_0 = 0.1$, $\phi = 0$ over a long period of sampling window with $N = 2048$ and $n_0 = -N/2$. In this case, the sampling interval is $\Delta T = 1$ which gives the non-aliasing angular frequency range $[-\pi, \pi)$. As shown in Fig. 12, the frequencies at both ends of the time indices exceed the non-aliasing frequency range and hence are wrapped back to the fundamental frequency range.

The proposed estimator used the extracted IF from Fig. 12 (b) and (26) to unwrap it for the subsequent refining estimation stages. The measured MSEs for the proposed estimator are shown in Fig. 13. It is seen that the proposed estimator can correctly unwrap the aliased frequency spectra and converge the estimation performance towards the CRB. On the other hand, the PULS estimator didn't take into account the aliasing effect and, as a result, we exclude the PULS estimator here.
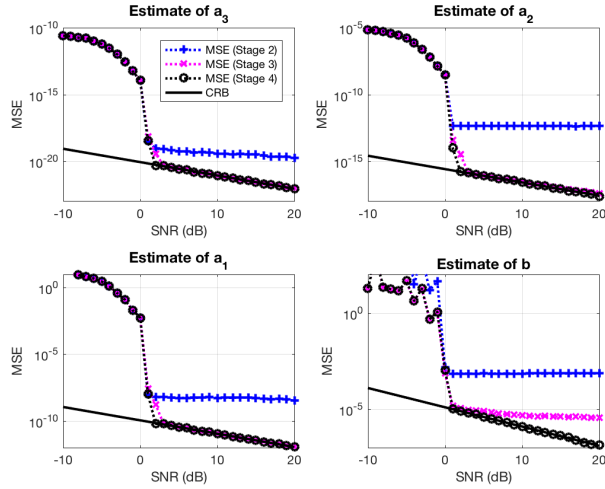
Figure 13: Measured MSEs for the proposed estimator for the aliasing case in Fig. 12.

6. Conclusion

In this paper, a robust three-stage estimation scheme has been proposed for parameter estimation of coupled mixture of PPS and sinusoidal FM signal. It deals with issues such as performance at low SNRs and the aliasing effect, which have not been fully addressed by existing approaches. The initial parameter estimates are obtained by a combination of the polynomial regression and nonlinear optimization of IF estimates, extracted by the STFT due to its robustness to the noise. While the STFT-based IF estimates are biased, the subsequent refining stages iteratively reduces the STFT-induced estimation bias by low-pass filtering the demodulated narrowband signal with initial estimates from the first stage. The final estimate is produced by the Nedler-Mead simplex nonlinear optimization algorithm. Extensive Monte-Carlo performance evaluation in various scenarios shows that the proposed method can significantly lower the SNR threshold than the phase-based PULS approach and the measured MSEs approach to corresponding CRBs as the proposed estimator moves from the initial stage to the final refining stages.

References

[1] S. Peleg and B. Friedlander, "The discrete polynomial-phase transform," *IEEE Trans. on Signal Processing*, vol. 43, no. 8, pp. 1901–1914, Aug. 1995.

[2] S. Peleg and B. Friedlander, "Multicomponent signal analysis using the polynomial-phase transform," *IEEE Trans. Aerosp. Electron. Syst.*, vol. 32, no. 1, pp. 378–387, Jan 1996.

[3] S. Barbarossa and V. Petrone, "Analysis of polynomial-phase signals by the integrated generalized ambiguity function," *IEEE Trans. on Signal Processing*, vol. 45, no. 2, pp. 316–327, Feb. 1997.

[4] B. Ristic and B. Boashash, "Comments on "the Cramér-Rao lower bounds for signals with constant amplitude and polynomial phase"," *IEEE Trans. on Signal Processing*, vol. 46, no. 6, pp. 1708–1709, June 1998.

[5] P. O'Shea, "A fast algorithm for estimating the parameters of a quadratic FM signal," *IEEE Trans. on Signal Processing*, vol. 52, no. 2, pp. 385–393, Feb. 2004.

[6] D. S. Pham and A. M. Zoubir, "Analysis of multicomponent polynomial phase signals," *IEEE Trans. on Signal Processing*, vol. 55, no. 1, pp. 56–65, Jan 2007.

[7] P. Wang, I. Djurović, and J. Yang, "Generalized high-order phase function for parameter estimation of polynomial phase signal," *IEEE Trans. on Signal Processing*, vol. 56, no. 7, pp. 3023–3028, July 2008.

[8] P. Wang, I. Djurović, and J. Yang, "Modifications of the cubic phase function," *Chinese Journal of Electronics*, vol. 17, no. 1, pp. 189–194, January 2008.

[9] P. Wang, H. Li, I. Djurović, and B. Himed, "Instantaneous frequency rate estimation for high-order polynomial-phase signals," *IEEE Signal Processing Letters*, vol. 16, no. 9, pp. 782–785, September 2009.

[10] P. Wang, H. Li, I. Djurović, and B. Himed, "Integrated cubic phase function for linear FM signal analysis," *IEEE Trans. Aerosp. Electron. Syst.*, vol. 46, no. 3, pp. 963–977, July 2010.

[11] R. G. McKilliam and I. V. L. Clarkson, "Identifiability and aliasing in polynomial-phase signals," *IEEE Trans. on Signal Processing*, vol. 57, no. 11, pp. 4554–4557, Nov 2009.

[12] A. Amar, A. Leshem, and A. J. van der Veen, "A low complexity blind estimator of narrowband polynomial phase signals," *IEEE Trans. on Signal Processing*, vol. 58, no. 9, pp. 4674–4683, Sep 2010.

[13] I. Djurović, M. Simeunović, S. Djukanović, and P. Wang, "A hybrid CPF-HAF estimation of polynomial-phase signals: Detailed statistical analysis," *IEEE Trans. on Signal Processing*, vol. 60, no. 10, pp. 5010–5023, Oct. 2012.

[14] I. Djurović, S. Djukanović, and V. V. Lukin, "An algorithm for the fine estimation of polynomial-phase signals," *IEEE Trans. Aerosp. Electron. Syst.*, vol. 48, no. 4, pp. 3687–3693, October 2012.

[15] I. Djurović and M. Simeunović, "Resolving aliasing effect in the QML estimation of PPSs," *IEEE Trans. Aerosp. Electron. Syst.*, vol. 52, no. 3, pp. 1494–1499, June 2016.

[16] G. T. Zhou and Y. Wang, "Exploring lag diversity in the high-order ambiguity function for polynomial phase signals," *IEEE Signal Processing Letters*, vol. 4, no. 8, pp. 189–194, Aug. 1997.

[17] M. Farquharson, P. O'Shea, and G. Ledwich, "A computationally efficient technique for estimating the parameters of polynomial phase signals from noisy observations," *IEEE Trans. on Signal Processing*, vol. 53, no. 8, pp. 3337–3342, Aug. 2005.

[18] J.-E. Wilbur and R. J. McDonald, "Nonlinear analysis of cyclically correlated spectral spreading in modulated signals," *J. Acoust. Soc. Amer.*, vol. 92, pp. 219–230, July 1992.

[19] M. R. Bell and R. A. Grubbs, "JEM modeling and measurement for radar target identification," *IEEE Trans. Aerosp. Electron. Syst.*, vol. 29, pp. 73–87, Jan. 1993.

[20] S. Palumbo, S. Barbarossa, A. Farina, and M. R. Toma, "Classification techniques of radar signals backscattered by helicopter blades," in *Proceedings of Int. Symp. Digital Signal Process.*, London, UK, July 1996.

[21] F. Gini and G. B. Giannakis, "Parameter estimation of hybrid hyperbolic FM and polynomial phase signals using the multi-lag high-order ambiguity function," in *Proceedings of The Thirty-First Asilomar Conference on Signals, Systems, and Computers*, Nov. 1997, vol. 1, pp. 250–254.

[22] F. Gini and G. B. Giannakis, "Hybrid FM-polynomial phase signal modeling: Parameter estimation and Cramér-Rao bounds," *IEEE Trans. on Signal Processing*, vol. 47, no. 2, pp. 363–377, Feb. 1999.

[23] P. Wang, P. V. Orlik, K. Sadamoto, W. Tsujita, and F. Gini, "Parameter estimation of hybrid sinusoidal FM-polynomial phase signal," *IEEE Signal Processing Letters*, vol. 24, no. 1, pp. 66–70, Jan 2017.

[24] P. Wang, P. V. Orlik, K. Sadamoto, W. Tsujita, and Y. Sawa, "Cramér-Rao bounds for a coupled mixture of polynomial phase and sinusoidal FM signals," *IEEE Signal Processing Letters*, vol. 24, no. 6, pp. 66–70, June 2017.

[25] P. Wang, P. V. Orlik, B. Wang, K. Sadamoto, W. Tsujita, and Y. Sawa, "Speed estimation of contactless electromagnetic encoders," in *Proceedings of the 43rd Annual Conference of the IEEE Industrial Electronics Society (IECON'17)*, Beijing, China, Nov. 2017.

[26] J. F. Gieras, Z. J. Piech, and B. Tomczuk, *Linear Synchronous Motors: Transportation and Automation Systems*, CRC Press, Boca Raton, FL, 2011.

[27] B. M. Wilamowski and J. D. Irwin, *The Industrial Electronics Handbook*, CRC Press, Boca Raton, FL, 2011.

[28] S. Valiviita and S. J. Ovaska, "Delayless acceleration measurement method for elevator control," *IEEE Transactions on Industrial Electronics*, vol. 45, no. 2, pp. 364–366, Apr 1998.

[29] S. Valiviita and S. J. Ovaska, "Delayless recursive differentiator with efficient noise attenuation for motion control applications," in *Proceedings of the 24th Annual Conference of the IEEE Industrial Electronics Society (IECON'98)*, Aug 1998, vol. 3, pp. 1481 – 1486.

[30] S. Valiviita, S. J. Ovaska, and O. Vainio, "Polynomial predictive filtering in control instrumentation: a review," *IEEE Transactions on Industrial Electronics*, vol. 46, no. 5, pp. 876–888, Oct 1999.

[31] I. Djurović, M. Simeunović, and P. Wang, "Cubic phase function: A simple solution for polynomial phase signal analysis," *Signal Processing*, vol. 135, pp. 48–66, June 2017.

[32] I. Djurović, M. Simeunović, and B. Lutovac, "Are genetic algorithms useful for the parameter estimation of FM signals," *Digital Signal Processing*, vol. 22, no. 6, pp. 1137–1144, Nov. 2012.

[33] I. Djurović, C. Ioana, T. Thayaparan, LJ. Stanković, P. Wang, V. Popović, and M. Simeunović, "Cubic phase function

evaluation for multicomponent signals with application to SAR imaging," *IET Signal Processing*, vol. 4, no. 4, pp. 371–381, Aug. 2010.

[34] P. O'Shea, "On refining polynomial phase signal parameter estimates," *IEEE Trans. Aerosp. Electron. Syst.*, vol. 46, no. 3, pp. 978–987, July 2010.

[35] I. Djurović and LJ. Stanković, "STFT-based estimator of polynomial phase signals," *Signal Processing*, vol. 2012, no. 11, pp. 2769–2774, Nov. 2012.

[36] I. Djurović and LJ. Stanković, "Quasi maximum likelihood estimator of polynomial phase signals," *IET Signal Processing*, vol. 13, no. 4, pp. 347–359, June 2014.

[37] I. Djurović, "On parameters of the QML PPS estimator," *Signal Processing*, vol. 116, no. 11, pp. 1–6, Nov. 2015.

[38] I. Djurović and M. Simeunović, "The STFT-based estimator of micro-Doppler parameters," *Digital signal processing*, vol. 72, no. 1, pp. 59–74, June 2018.

[39] LJ. Stanković, I. Djurović, S. Stanković, M. Simeunović, and M. Daković, "Instantaneous frequency in time-frequency analysis: Enhanced concepts and performance of estimation algorithms," *Digital Signal Processing*, vol. 35, no. 4, pp. 1–13, Dec. 2014.

[40] B. Boashash, *Time frequency signal analysis and processing: a comprehensive reference*, Academic Press, Elsevier, 2015.

[41] M. Mesbah, J. O'Toole, P. Colditz, and B. Boashash, "Instantaneous frequency based newborn EEG seizures characterization," *EURASIP Journal on Advances in Signal Processing*, vol. 2012, no. 1, pp. 1–13, July 2012.

[42] J. Lerga and V. Sucić, "Nonlinear IF estimation based on the pseudo WVD adapted using the improved sliding pairwise ICI rule," *IEEE Signal Processing Letters*, vol. 16, no. 11, pp. 953–956, Nov. 2009.

[43] B. Guo, S. Peng, X. Hu, and P. Xu, "Complex-valued dierential operator-based method for multi-component signal separation," *Signal processing*, vol. 132, pp. 66–76, March 2017.

[44] I. Djurović, V. Popović-Bugarin, and M. Simeunović, "The STFT-based estimator of micro-Doppler parameters," *IEEE Trans. Aerosp. Electron. Syst.*, vol. 53, no. 3, pp. 1273–1283, June 2017.

[45] J. A. Legg and D. A. Gray, "Performance bounds for polynomial phase parameter estimation with non-uniform and random sampling schemes," *IEEE Trans. on Signal Processing*, vol. 48, no. 2, pp. 331–337, Feb. 2000.

[46] J. Angeby, "Aliasing of polynomial-phase signal parameters," *IEEE Trans. on Signal Processing*, vol. 48, no. 5, pp. 1448–1491, May 2000.